Structural effect on the resistive switching behavior of triphenylamine-based poly(azomethine)s†

Wenbin Zhang,‡[ab] Cheng Wang,‡[c] Gang Liu,*[a] Jun Wang,[b] Yu Chen*[c] and Run-Wei Li*[a]

Linear and hyperbranched poly(azomethine)s (PAMs)-based on triphenylamine moieties are synthesized and used as the functioning layers in the Ta/PAM/Pt resistive switching memory devices. Comparably, the hyperbranched PAM with isotropic architecture and semi-crystalline nature shows enhanced memory behaviors with more uniform distribution of the HRS and LRS resistances.

By providing inexpensive, lightweight, optically transparent and CMOS compatible modules on mechanically flexible plastic substrates, polymer memories have demonstrated great potential as information storage components in current consumer digital gadgets.[1] Rather than encoding '0' and '1' as the amount of charges stored in a silicon cell, resistive switching memory stores data in a different matter, for instance, based on the high and low resistance states (HRS and LRS) of a metal/insulator/metal structure in response to the external electric field.[2]

Various polymers, including conjugated polymers, polymers with pendent chromophores, and donor–acceptor polymers, have been demonstrated to have memory switching characteristics.[3] Similar to the other organic electronic devices, most of the polymers used in memories are linear in structure. In contrast to the linear counterparts, hyperbranched polymers exhibit unique three dimensional structures, good solubility, low melting temperature and solution viscosity, and excellent physiochemical properties.[4] More importantly, the charge carrier transport, which was found to be anisotropic and strongly depends on the orientation and packing mode of the molecules, can be efficiently enhanced in the isotropic architecture of the hyperbranched polymers.[5] With its propeller like geometry with a dihedral angle of around 120° between the phenyl rings connected to the central nitrogen atom, triphenylamine (TPA) molecule is considered as an interesting building block to construct hyperbranched conjugated polymers for electronic applications.

Aromatic poly(azomethine)s (PAMs) are a class of materials composed of azomethine (C═N) unities and benzene rings alternatively in the backbone and possess the merits of easy molecular design and synthesis, good thermal stability, excellent mechanical strength, ability to form metal chelates, liquid crystalline properties and non-linear optical properties.[6] In this work, conjugated linear and hyperbranched PAMs with triphenylamine chromophores in the polymer backbone have been synthesized *via* comparatively convenient one step condensation polymerization of aldehydes and amines (see Scheme 1, Scheme S1 and ESI† for the detailed synthesis and characterization), and the structural effect on their memory switching behaviors have been comparably investigated.

The building blocks of the linear and hyperbranched PAMs are chemically identical, except for the spatial arrangement of the triphenylamine chromophores. The structures of the as-synthesized PAMs were confirmed by ^{1}H nuclear magnetic resonance (^{1}H NMR) and Fourier transform infrared (FTIR). The ^{1}H NMR signals with the

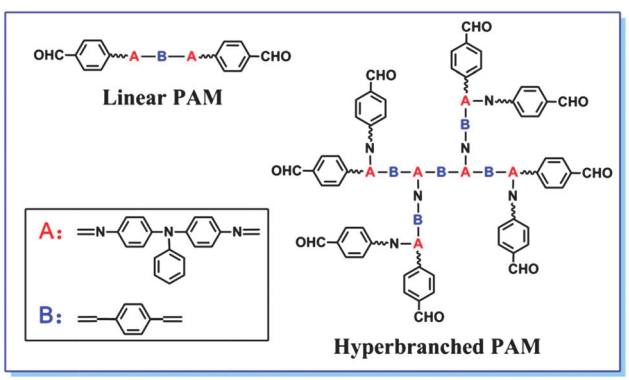

Scheme 1 Molecular structures of the linear and hyperbranched PAMs.

[a] *Key Laboratory of Magnetic Materials and Devices, Zhejiang Province Key Laboratory of Magnetic Materials and Application Technology, Ningbo Institute of Materials Technology and Engineering, Chinese Academy of Sciences, Ningbo, 315201, P. R. China. E-mail: liug@nimte.ac.cn, runweili@nimte.ac.cn*

[b] *Department of Physics, Ningbo University, Ningbo 315211, China*

[c] *Institute of Applied Chemistry, East China University of Science and Technology, Shanghai, 200237, China. E-mail: chentangyu@yahoo.com*

† Electronic supplementary information (ESI) available. See DOI: 10.1039/c4cc05233a

‡ These authors contribute equally to this work.

chemical shifts of 8.1–7.9 ppm (linear PAM) and 8.2–7.9 ppm (hyperbranched PAM) correspond to the proton resonance of the C═N groups in respective PAMs. The signals at 7.4–7.0 ppm are ascribed to the protons on the aromatic rings of the triphenylamine moieties.[7] In the FTIR spectra, the absorption peaks at 1618 cm^{-1} and 1583 cm^{-1} are ascribed to the formation of C═N groups (Fig. S1 of ESI†).[7b] Due to the presence of triphenylamine chromophores in the main chains, both the linear and hyperbranched PAMs show good solubilities in common polar organic solvents of tetrahydrofuran, methylene chloride, chloroform, *N*-methyl pyrrolidone and dimethyl formamide.[7b] The number-average molecular weight (M_n) of the linear and hyperbranched PAMs are 5.1×10^3 and 3.6×10^3, respectively. GPC traces of the two PAMs are shown in Fig. S2 of ESI.† In comparison to that of the linear PAM, the GPC trace of the hyperbranched PAM is narrower, which implies its more uniform molecular weight distribution. The UV-Visible absorption spectra of PAMs, which show absorption bands of the π–π* transition of the conjugated backbone at the shorter wavelength region and the coupling between the n–π* and π–π* transitions of the arylamine moieties at the longer wavelength region, respectively, are displayed in Fig. S3 (ESI†). Both PAMs exhibit excellent thermal stability with the onset decomposition (10% weight loss) temperatures of 470 °C and 458 °C, respectively (Fig. S4, ESI†). The onset oxidation potentials for the linear and hyperbranched PAMs are 0.86 V and 0.90 V, leading to the HOMO–LUMO energy levels of −5.28 eV/−2.85 eV and −5.32 eV/−2.93 eV, respectively (Fig. S5 of ESI†).

X-ray diffraction (XRD) techniques have been used to check the crystallinity of the two PAMs (Fig. 1). In good agreement with the reported literature, linear PAM is amorphous with broad diffractive peaks in the 2θ range of 5°–90°.[5] In obvious contrast, the hyperbranched PAM is semi-crystalline with diffractive peaks at $2\theta = 20°$, 24°, and 30°, respectively. Transmission electron microscopic (TEM) images of the linear and hyperbranched PAMs are also shown in Fig. 1c and d, respectively. Apparently, the linear PAM is non-crystalline, while the hyperbranched counterpart shows localized crystalline regions.[8] We also investigate the topographies of the PAM films by atomic force microscopy (AFM) technique in a tapping mode before depositing top electrodes. Fig. 1e and f show 2 μm × 2 μm AFM images of the linear and hyperbranched PAMs, respectively. The linear PAM clearly shows uneven morphology of a

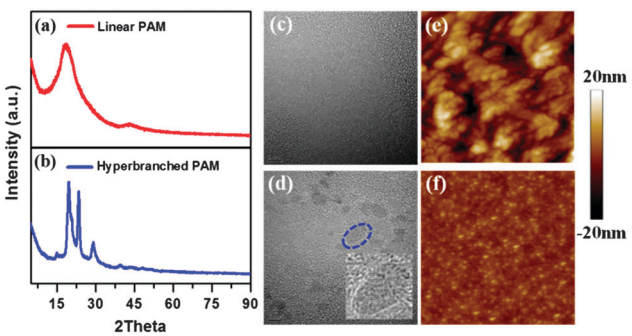

Fig. 1 X-ray diffractive patterns of the (a) linear and (b) hyperbranched PAMs powders. TEM and AFM images of the (c, e) linear and (d, f) hyperbranched PAM films, respectively.

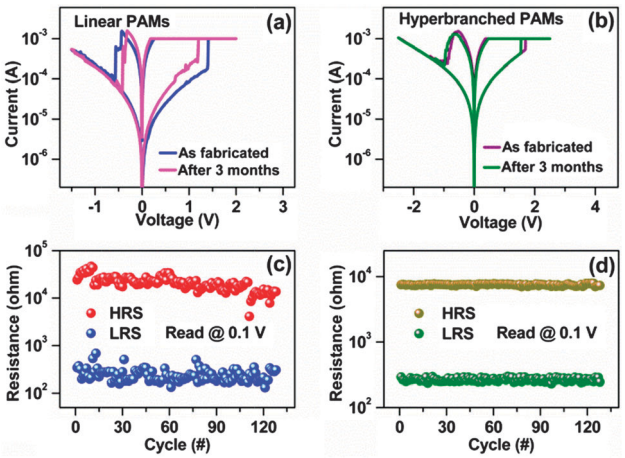

Fig. 2 The current–voltage switching and endurance performance of the Ta/PAM/Pt memory devices fabricated with the (a, c) linear and (b, d) hyperbranched PAMs, respectively.

rod-like structure, which probably arises from the irregular agglomeration of the polymer chains into wool balls.[9] On the other hand, the hyperbranched PAM, which possesses relatively less polymer chain folding with larger steric hindrance displays a uniform nanofilm. Meanwhile, the surface root-mean-square roughness of the hyperbranched PAM film is smaller (0.76 nm) than that of the linear PAM film (1.23 nm).

The resistive switching performances of the two PAMs are demonstrated by the current–voltage characteristics of the Ta/PAM/Pt structured devices (Fig. 2). A compliance current of 10^{-3} A has been preset to avoid device breakdown from overstriking. It is found that the forming operations are always necessary for both polymer devices to be set to the LRS for the first time (Fig. S6 of ESI†). Afterwards, a negative voltage of −0.41 V can reset the linear PAM device to HRS, while a subsequent positive sweep of 1.40 V can set the linear PAM device to the LRS again (Fig. 2a). The HRS to LRS transition can be defined as the "set" or "write" process, and accordingly, the LRS to HRS transition is defined as the "reset" or "erase" process. Both the HRS and LRS can be read nondestructively and are stable after removing the power supply, thus completing the "forming-read-erasing-rewriting" cycles of a non-volatile memory with a ON/OFF ratio over 10^2. The linear PAM device behaves similarly after being left in air for three months, except for a notable change in the device resistance and the switching voltages. In comparison, the hyperbranched PAM can be set and reset with the sweeping voltages of 1.73 V and −0.53 V, respectively, and its resistive switching behavior can be reproduced with good accuracy after three months (Fig. 2b).

The endurance performance of the Ta/PAM/Pt was also evaluated in ambient atmosphere by cyclic switching operations. Fig. 2c and d show the evolution of the linear and hyperbranched PAM device resistances in the first 128 cycles, respectively. The resistance values in each DC sweep were read at 0.1 V. For the Ta/linear PAM/Pt stacks, the HRS resistance rapidly decreases while the LRS resistance fluctuates in less than one order of magnitude. For the Ta/hyperbranched PAM/Pt memory devices, much more

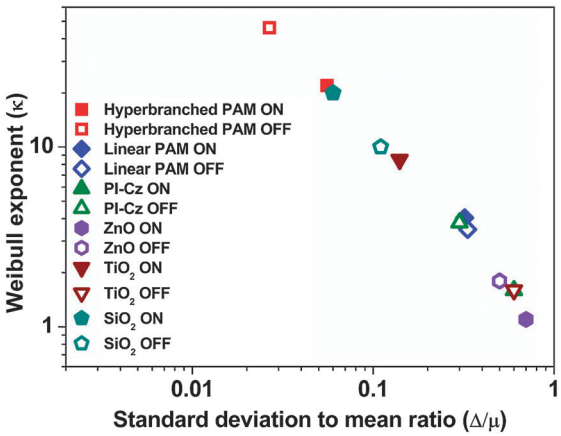

Fig. 3 Weibull exponent (*k*) *versus* standard deviation to mean ratio (Δ/μ) for the HRS and LRS resistances of the PAM and other reported devices.

uniform distribution of the HRS and LRS resistances are observed. We also count the resistance values of HRS and LRS in all the switching cycles. As expected, a narrow distribution of R_{HRS} (7.5 ± 0.2 kΩ) and R_{LRS} (270 ± 15 Ω) are obtained in the Ta/hyperbranched PAM/Pt memory, while the resistance values of Ta/linear PAM/Pt exhibit relatively fluctuated distribution range of 21 ± 7 kΩ (R_{HRS}) and 250 ± 80 Ω (R_{LRS}). We have also used Weibull analysis to further quantify the uniformity of the PAM devices (details can be found in ESI†). Generally, the larger Weibull exponent (k) and smaller standard deviation (Δ) to mean (μ) ratio (Δ/μ) correspond to superior uniformity of the parameters under evaluation.[10] For the Pt/linear PAM/Ta stack, the Δ/μ values of the HRS and LRS resistances are 0.3200 and 0.3333, respectively. In contrast, the HRS and LRS resistances of the hyperbranched PAM device feature smaller Δ/μ values of 0.0267 and 0.0556, respectively. Fig. 3 summarizes the Weibull component k of the HRS and LRS resistances of the PAM and other reported devices, as a function of the standard deviation Δ/μ.[11] The Ta/hyperbranched PAM/Pt device exhibits the highest k and lowest Δ/μ, which even exceeds the performance of inorganic counterparts. Pulse switching operations were conducted with a write–read–erase–rewrite (WRER) sequence to further study the endurance performance of the PAM devices. The set/reset voltages of the linear and hyperbranched PAMs are 4.0 V/−2.0 V and 3.0 V/−2 V, respectively, while the duration of the voltage pulse applied to the Ta/PAM/Pt memory devices is 2 μs. The read voltages for both devices are 0.1 V. The memory performance based on these two PAMs is found to be stable for over 5000 WRER cycles (Fig. S7 of ESI†). Fig. S8 (ESI†) shows the retention capability of the Ta/PAM/Pt memory devices in their LRS and HRS, respectively. The maintenance of the HRS and LRS in the hyperbranched PAM device under 0.1 V constant voltage stress for 1×10^4 s, suggests that the superior device performance may be obtained by utilizing polymers with hyperbranched structure in thin film devices.

The resistive switching mechanism of the Ta/PAM/Pt memory devices can be attributed to the charge trapping and detrapping in the PAM backbones.[12] As shown in Scheme 1, the terminal aldehyde groups and nitrogen atoms of the azomethine and triphenylamine chromophores may act as the nucleophilic and electrophilic trapping site, respectively.[7b,12a] When a positive voltage with sufficient amplitude is applied, the traps will become fully filled with holes. The subsequently injected holes from the electrode can migrate more freely in the polymer thin film and switch the device from HRS to LRS. With the enhanced isotropic architecture in the hyperbranched PAM thin films, charge carrier transport becomes more efficient and stable, which accounts for the superior switching performance in the Ta/PAM/Pt devices.[11e] When the negative reset voltage is applied to the devices, the filled traps are detrapped to regenerate the potential well for charge carrier hopping and switch the device back to HRS.[12a]

In summary, linear and hyperbranched PAMs with identical chemical structure but different molecular geometries and crystalline qualities have been successfully synthesized *via* condensation polymerization and explored for resistive switching performance. Both polymer exhibit smaller switching voltages of −0.41 V/1.4 V and −0.53 V/1.73 V, ON/OFF ratios over 100, endurance capability for more than 5000 cycles and retention time exceeding 10^4 s. In comparison, the hyperbranched PAM thin film with isotropic architecture demonstrates uniform distribution of the HRS and LRS resistances, which is beneficial for practical memory device applications.

The authors acknowledge the financial supports from the State Key Project of Fundamental Research of China (973 Program, 2012CB933004), National Natural Science Foundation of China (51303194, 11274321, 61328402, 21074034), Ningbo Science and Technology Innovation Team (2011B82004), Ningbo Natural Science Foundations (2013A610031).

Notes and references

1 (*a*) Emerging research devices. In: International Technology Roadmap for Semiconductors (ITRS) 2005 edn 1–70 (Semiconductor Industry Association, International Sematech, Austin, TX, 2005); (*b*) Q. D. Ling, D. J. Liaw, C. X. Zhu, D. S. H. Chan, E. T. Kang and K. G. Neoh, *Prog. Polym. Sci.*, 2008, **33**, 917.

2 (*a*) T. C. Chang, F. Y. Jian, S. C. Chen and Y. T. Tsai, *Mater. Today*, 2011, **14**, 608; (*b*) S. B. Long, C. Cagli, D. Ielmini, M. Liu and J. Sune, *J. Appl. Phys.*, 2012, **111**, 074508; (*c*) X. J. Zhu, W. J. Su, Y. W. Liu, B. L. Hu, L. Pan, W. Lu, J. D. Zhang and R.-W. Li, *Adv. Mater.*, 2012, **24**, 3941; (*d*) J. Shang, G. Liu, H. L. Yang, X. J. Zhu, X. X. Chen, H. W. Tan, B. L. Hu, L. Pan, W. H. Xue and R.-W. Li, *Adv. Funct. Mater.*, 2014, **24**, 2171.

3 (*a*) G. Liu, B. Zhang, Y. Chen, C. X. Zhu, L. J. Zeng, D. S. H. Chan, K. G. Neoh, J. N. Chen and E. T. Kang, *J. Mater. Chem.*, 2011, **21**, 6027; (*b*) K. L. Wang, Y. L. Liu, J. W. Lee, K. G. Neoh and E. T. Kang, *Macromolecules*, 2010, **43**, 7159; (*c*) H. C. Wu, A. D. Yu, W. Y. Lee, C. L. Liu and W. C. Chen, *Chem. Commun.*, 2012, **48**, 9135; (*d*) D. J. Liaw, K. L. Wang, Y. C. Huang, K. R. Lee, J. Y. Lai and C. S. Ha, *Prog. Polym. Sci.*, 2012, **37**, 907; (*e*) J. H. Wu, H. J. Yen, Y. C. Hu and G. S. Liou, *Chem. Commun.*, 2014, **50**, 4915.

4 (*a*) J. M. J. Fréchet, *Science*, 1994, **263**, 1710; (*b*) X. T. Tao, Y. D. Zhang, T. Wada, H. Sasabe, H. Suzuki, T. Watanabe and S. Miyata, *Adv. Mater.*, 1998, **10**, 226; (*c*) X. M. Liu, C. B. He, X. T. Hao, L. W. Tan, Y. Q. Li and K. S. Ong, *Macromolecules*, 2004, **37**, 5965.

5 (*a*) H. Sirringhaus, P. J. Brown, R. H. Friend, M. M. Nielsen, K. Bechgaard, B. M. W. Langeveld-Voss, A. J. H. Spiering, R. A. J. Janssen, E. W. Meijer and P. Herwig, *et al.*, *Nature*, 1999, **401**, 685; (*b*) H. Yang, T. J. Shin, L. Yang, K. Cho, C. Y. Ryu and Z. Bao, *Adv. Funct. Mater.*, 2005, **15**, 671; (*c*) J. Roncali, P. Leriche and A. Cravino, *Adv. Mater.*, 2007, **19**, 2045.

6 (*a*) L. Pan, B. L. Hu, X. J. Zhu, X. X. Chen, J. Shang, H. W. Tan, W. H. Xue, Y. J. Zhu, G. Liu and R.-W. Li, *J. Mater. Chem. C*, 2013, **1**, 4556; (*b*) B. L. Hu,

X. J. Zhu, X. X. Chen, L. Pan, S. S. Peng, Y. Z. Wu, J. Shang, G. Liu, Q. Yan and R.-W. Li, *J. Am. Chem. Soc.*, 2012, **134**, 17408; (*c*) M. A. Khalid, A. G. El-Shekeil and F. A. Al-Yusufy, *Eur. Polym. J.*, 2001, **37**, 1423; (*d*) L. Song, C. L. Tu, Y. F. Shi, F. Qiu, L. He, Y. Jiang, Q. Zhu, B. S. Zhu, D. Y. Yan and X. Y. Zhu, *Macromol. Rapid Commun.*, 2010, **31**, 443.

7 (*a*) H. J. Niu, P. H. Luo, M. L. Zhang, L. Zhang, L. N. Hao, J. Luo, X. D. Bai and W. Wang, *Eur. Polym. J.*, 2009, **45**, 3058; (*b*) H. J. Niu, Y. D. Huang, Y. D. Bai, X. Li and G. L. Zhang, *Mater. Chem. Phys.*, 2004, **86**, 33.

8 (*a*) F. Ania, F. J. Balta-Calleja, A. Flores, G. H. Michler, S. Scholtyssek, D. Khariwala, A. Hiltner, E. Baer, L. Rong and B. S. Hsiao, *Eur. Polym. J.*, 2012, **48**, 86; (*b*) G. Shen, V. A. Piunova, S. Nutt and T. E. Hogen-Esch, *Polymer*, 2013, **54**, 5790.

9 (*a*) J. N. L. Albert, W. S. Young, R. L. Lewis, T. D. Bogart, J. R. Smith and T. H. Epps, *ACS Nano*, 2012, **6**, 459; (*b*) J. A. Yoon, T. Young, K. Matyjaszewski and T. Kowalewski, *ACS Appl. Mater. Interfaces*, 2010, **2**, 2475; (*c*) C. J. Lu, Q. Liu, P. Y. Gu, D. Y. Chen, F. Zhou, H. Li, Q. F. Xu and J. M. Lu, *Polym. Chem.*, 2014, **5**, 2602.

10 (*a*) W. Weibull, *J. Appl. Mech.*, 1951, **18**, 293; (*b*) S. B. Long, X. J. Lian, C. Cagli, L. Perniola, E. Miranda, M. Liu and J. Sune, *IEEE Electron Device Lett.*, 2013, **34**, 999.

11 (*a*) B. J. Choi, A. B. K. Chen, X. Yang and I. W. Chen, *Adv. Mater.*, 2011, **23**, 3847; (*b*) W. Y. Chang, K. J. Cheng, J. M. Tsai, H. J. Chen, F. Chen, M. J. Tsai and T. B. Wu, *Appl. Phys. Lett.*, 2009, **95**, 3; (*c*) B. L. Hu, F. Zhuge, X. J. Zhu, S. S. Peng, X. X. Chen, L. Pan, Q. Yan and R. W. Li, *J. Mater. Chem.*, 2012, **22**, 520; (*d*) Y. C. Yang, F. Pan, Q. Liu, M. Liu and F. Zeng, *Nano Lett.*, 2009, **9**, 1636; (*e*) D. C. Kim, M. J. Lee, S. E. Ahn, S. Seo, J. C. Park, I. K. Yoo, I. G. Baek, H. J. Kim, E. K. Yim, J. E. Lee, S. O. Park, H. S. Kim, U. I. Chung, J. T. Moon and B. I. Ryu, *Appl. Phys. Lett.*, 2006, **88**, 3.

12 (*a*) S. H. Hong, O. Kim, S. Choi and M. Ree, *Appl. Phys. Lett.*, 2007, **91**, 3; (*b*) J. Y. Ouyang, *Appl. Phys. Lett.*, 2013, **103**, 4; (*c*) R. T. Weitz, A. Walter, R. Engl, R. Sezi and C. Dehm, *Nano Lett.*, 2006, **6**, 2810; (*d*) R. J. Tseng, J. X. Huang, J. Ouyang, R. B. Kaner and Y. Yang, *Nano Lett.*, 2005, **5**, 1077.